Protection of Pancreatic Islets Using Theranostic Silencing Nanoparticles in a Baboon Model of Islet Transplantation

Thomas Pomposelli,[1] Ping Wang,[2,3] Kazuhiro Takeuchi,[1] Katsunori Miyake,[1] Yuichi Ariyoshi,[1] Hironosuke Watanabe,[1] Xiaojuan Chen,[1] Akira Shimizu,[1] Neil Robertson,[2,3] Kazuhiko Yamada,[1] and Anna Moore[2,3]

Diabetes 2020;69:2414–2422 | https://doi.org/10.2337/db20-0517

The long-term success of pancreatic islet transplantation (Tx) as a cure for type 1 diabetes remains limited. Islet loss after Tx related to apoptosis, inflammation, and other factors continues to limit Tx efficacy. In this project, we demonstrate a novel approach aimed at protecting islets before Tx in nonhuman primates (NHPs) (baboons) by silencing a gene (caspase-3) responsible for induction of apoptosis. This was done using siRNA (siCas-3) conjugated to magnetic nanoparticles (MNs). In addition to serving as carriers for siCas-3, these nanoparticles also act as reporters for MRI, so islets labeled with MN-siCas-3 can be monitored in vivo after Tx. In vitro studies showed the antiapoptotic effect of MN-siCas-3 on islets in culture, resulting in minimal islet loss. For in vivo studies, donor baboon islets were labeled with MN-siCas-3 and infused into recipient diabetic subjects. A dramatic reduction in insulin requirements was observed in animals transplanted with even a marginal number of labeled islets compared with controls. By demonstrating the protective effect of MN-siCas-3 in the challenging NHP model, this study proposes a novel strategy to minimize the number of donor islets required from either cadaveric or living donors.

The long-term success of pancreatic islet transplantation (Tx) remains frustratingly limited (1,2), although initially, it gained momentum as a possible alternative to en bloc pancreas Tx because of the relative safety of the procedure (3). Even with the immunosuppressive regimen known as the Edmonton protocol, insulin independence was only transient in most recipients because of significant islet loss that starts early after the procedure (1). Consequentially, a long-term follow-up of the patients revealed that ∼75% required exogenous insulin at 2 years after Tx (2). Since then, other centers also reported mixed rates of success (4).

The reasons for the limited long-term success of islet Tx are multifactorial and include immunological as well as nonimmunological events, such as instant blood-mediated inflammatory reaction, ischemia-induced islet apoptosis, recurrence of autoimmunity, and allogeneic immune rejection (5–14). The latter requires permanent use of immunosuppressive drugs, such as in the Edmonton protocol (daclizumab, rapamycin, and tacrolimus). However, studies have demonstrated that these drugs are far from safe. As such, rapamycin, a key component of this regimen, impairs glucose tolerance and β-cell proliferation of transplanted and host islets (15,16), reduces glucose-stimulated insulin secretion, and reversibly decreases β-cell replication (15). Moreover, there is direct evidence that this therapy leads to re-emergence of autoreactivity, the condition that Tx is supposed to treat. Studies also demonstrated that Tx using the Edmonton protocol in patients with type 1 diabetes results in lymphopenia associated with elevated homeostatic cytokines and expansion of autoreactive $CD8^+$ T cells (17). Besides having a negative effect on transplanted grafts, immunosuppressants put

[1]Columbia Center for Translational Immunology, Columbia University Medical Center, New York, NY
[2]Precision Health Program, Michigan State University, East Lansing, MI
[3]Department of Radiology, College of Human Medicine, Michigan State University, East Lansing, MI

Corresponding authors: Anna Moore, moorea57@msu.edu, and Kazuhiko Yamada, KY2323@cumc.columbia.edu

Received 18 May 2020 and accepted 24 August 2020

This article contains supplementary material online at https://doi.org/10.2337/figshare.12857708.

T.P. and P.W. contributed equally to this study as first authors.

A.M. and K.Y. contributed equally to this study as senior authors.

patients at greater risk for developing certain cancers and increase susceptibility to infection (18). Additionally, the functionality of regulatory T cells promoting long-term graft acceptance may be impaired, while several drugs used in clinical practice affect islet engraftment, revascularization, and β-cell function (19–21). Lack of established vasculature leads to deprivation of nutrients and oxygen to the islets, resulting in severe apoptosis (10,22) and inefficient utilization of precious donor material. In fact, islet Tx protocols usually require up to 10,000 islet equivalents (IEQ)/kg to achieve insulin independence, often necessitating the use of two to three donor pancreata for a single recipient (10,22,23). Therefore, the success of islet Tx greatly depends on minimizing apoptotic islet death during the first weeks after Tx.

RNA interference offers great potential for therapeutic gene silencing and could be used for improving islet graft resistance to damaging factors after Tx. Previously, we have demonstrated the feasibility of inducing gene silencing using siRNA-conjugated iron oxide–based magnetic nanoparticle (MN-siRNA) probes. In addition to their ability to carry conjugated siRNA to pancreatic islets before Tx, magnetic properties of these nanoparticles allow for noninvasive monitoring of labeled islets after Tx in small and large animals (24–28). We also showed that nanoparticles conjugated to siRNAs directed toward genes responsible for islet damage were capable of silencing these genes before Tx, leading to protection of transplanted islet grafts in immunodeficient rodents (29–31). With the outlook to potential clinical translation of our studies and in search for a more efficient utilization of scarce donor islets, we performed studies in nonhuman primates (NHPs) using a marginal number of islets treated with MN-siRNA to a caspase-3 gene (MN-siCas-3) before Tx. Our choice of caspase-3 was dictated by the prominent role that this effector protein plays in initiation of the apoptotic cascade and mediation of cell death (23). Our results demonstrated a significant protective antiapoptotic effect of MN-siCas-3 on islets in culture, in vitro, and in vivo after Tx into recipient diabetic NHPs. We believe that our approach shows a potential for improving the outcome of islet Tx and reduction of islet donor requirements.

RESEARCH DESIGN AND METHODS

Probe Synthesis and Characterization

The double-stranded siRNAs targeting baboon caspase-3 (gene identifier: 101023728) was designed and synthesized by Eurogentec (Liege, Belgium) to incorporate a thiol group on the 5′ end of the sense strand. There was no modification of the antisense strand. The probe for islet labeling (MN-siCas-3) consisted of MNs conjugated to the near infrared fluorescence Cy5.5 dye and to siRNA to caspase-3 as previously described (30) (Fig. 1*A*). Briefly, dextran-coated iron oxide MNs were synthesized and labeled with a near infrared fluorescence Cy5.5 dye according to our previously established procedure (32). Their final size was 30 nm, with a zeta potential of 19 mV as determined by dynamic light scattering (Zetasizer; Malvern Panalytical, Westborough, MA). MN labeled with Cy5.5 was then conjugated to the heterobifunctional crosslinker N-succinimidyl 3-(2-pyridyldithio)propionate (Pierce Biotechnology, Rockford, IL) through the N-hydroxysuccinimide ester, followed by purification using a Sephadex G-25, PD-10 column. siRNA to caspase-3 was then conjugated to the nanoparticles through its 5′-sense thiol group. The amount of conjugated siRNA was assayed using agarose gel electrophoresis under reducing conditions (Tris-[carboxyethyl] phosphine hydrochloride). On average, we obtained seven to eight siRNA molecules per nanoparticle.

Animal Care, Diabetes Induction, and Study Design

All animal experiments were performed in compliance with institutional guidelines and were approved by the institutional animal care and use committee at Columbia University Medical Center and Michigan State University. Baboons (*Papio hamadryas*; Manheimer Foundation, Homestead, FL) were housed in an animal facility at the Columbia Center for Translational Immunology and quarantined for 6 weeks. All donors and recipients were MHC class I mismatched as proven by class I response assessed by interferon-γ enzyme-linked immunospot assays (33) (Supplementary Fig. 1). Recipient animals were six males and one female (4515) 25.3 ± 13.6 months old in the control group and 21.5 ± 13.1 in the experimental group (Table 1). There was no statistical difference in age between the two groups ($P = 0.73$). Donor animals were male except one (4015) in a control group. Age of donors was 46.4 ± 16.7 months in the control group and 50.0 ± 8.5 months in the experimental group. There was no statistical difference in age between the two groups ($P = 0.68$).

For diabetes induction, animals were injected intravenously with streptozotocin (STZ) (100 mg/kg) (Sigma, St. Louis, MO) through a peripheral line ~7–8 days before Tx (day −7) as we described before (30). For the first 24 h after STZ bolus, all animals displayed profound hypoglycemia caused by the lysis of their native islets with systemic release of insulin, often requiring multiple bolus doses of 50% dextrose. Next, with washout of native insulin, all animals displayed rising blood glucose requiring exogenous insulin within 48 h after STZ (Supplementary Fig. 2*A*). Thereafter, all animals displayed increasing levels of blood glucose, requiring >10 units of insulin a day (Supplementary Fig. 2*B*). All animals also displayed clinical signs of hyperglycemia and early diabetic ketoacidosis, including increased urination and acidosis. We were successful in inducing diabetes in all animals after one bolus of STZ, with the exception of animal 4515, which required two doses (Supplementary Fig. 2*B*). Animals were considered diabetic when fasting blood glucose levels were >250 mg/dL on 3 consecutive days. Diabetic baboons were then treated with injections of insulin guided by fasting blood glucose measurements. Our previous experience with baboons and rhesus macaques as well as the published literature

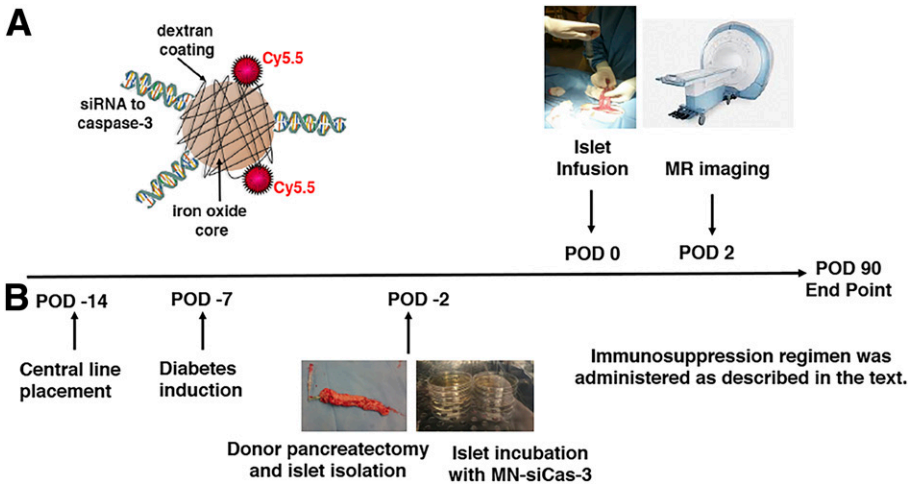

Figure 1—*A*: Schematic representation of MN-siCas-3 probe. The probe consisted of iron oxide nanoparticles conjugated to five Cy5.5 molecules and seven to eight molecules of siRNA to caspase-3. *B*: Timeline for the experimental and control groups. Diabetes was induced using STZ on POD −7. Donor pancreatectomy and islet isolation were performed on POD −2, followed by culture with the probes. On POD −1, the recipients underwent induction therapy and continued with the immunosuppression protocol throughout the course of the experiment. Islets were removed from culture on POD 0 and infused into the recipient's portal circulation.

indicate that 10 units/day of insulin is required to confirm successful induction of diabetes in these species (34,35). Analysis of C-peptide levels performed using ELISA (34) confirmed that STZ was successful in destroying the native islets (235.1 ± 53.1 pmol/L pre-STZ vs. 0.86 ± 2.1 pmol/L post-STZ).

Diabetic animals in experimental group ($n = 4$) received islets incubated with MN-siCas-3 before Tx, and diabetic animals in the control group ($n = 2$) received islets incubated with parental nanoparticles (MNs). One additional control animal (15P59) was rendered diabetic but did not receive islet infusion. Details describing experimental groups and the number of islets infused in each animal are shown in Table 1.

Donor Pancreatectomy and Islet Isolation

A detailed time course of the procedures in this study is shown in Fig. 1*B*. Complete pancreatectomy for islet isolation was performed on healthy donors ($n = 6$) 2 days before islet Tx (day −2) as we previously reported (35). For islet isolation, pancreata were infused with Liberase HI (Roche Biochemicals, Indianapolis, IN) and subjected to digestion followed by filtration through a mesh screen, application to a discontinuous gradient, and centrifugation (36). Islet purity and quantity was determined using standard dithizone staining (Sigma) while following manual islet counting according to O'Neil et al. (36). Purified islets were then cultured for 48 h in CMRL-1066 medium with 10% FBS and 100 mg/mL penicillin-streptomycin supplemented with the MN-siCas-3 or control probe (200 μg Fe/mL). After a 2-day culture, the islets were washed in CMRL-1066 medium, counted, and infused into the diabetic recipients.

Table 1—Experimental and control baboon groups indicating the number of infused islets and their treatment

Group	Baboon identifier	Probe treatment	Number of transplanted islets (IEQ/kg body weight)
Experimental	16P22	MN-siCas-3	7,600
Experimental	1315	MN-siCas-3	7,411
Experimental	15P38	MN-siCas-3	8,750
Experimental	8914	MN-siCas-3	6,650
Control	4515	MN	7,300
Control	16P46	MN	7,800
Control	15P59	NA	0

NA, not applicable.

In Vitro Studies

In vitro studies included quantitative evaluation of the islet yield after 48-h culture in the presence of experimental and control probes. In addition to the data from the donor islets used in the current study and to increase statistical significance of our results, we included additional data from islet isolations and culture that we performed for an unrelated study ($n = 3$/probe). We used a total of six preparations for the islets labeled with the experimental probe and five preparations for the islets labeled with the control probe. Each islet counting was performed in triplicate.

To evaluate the protective effects of MN-siCas-3 on pancreatic islets, the islets were cultured with the experimental or control probe at 200 μg Fe/mL for 48 h. This concentration has been shown to be sufficient to deliver enough siRNA molecules to cause major target downregulation (30,31). Evaluation of apoptosis in labeled islets was performed using an Apoptotic DNA Ladder Detection Kit (Merck, Darmstadt, Germany). Islets were lysed, and DNA was isolated and run through a 1% agarose gel at 95 V.

To confirm in vitro labeling of baboon islets with MN-siRNA probes we used immunohistology. Paraffin-embedded sections of labeled islets were incubated with rabbit polyclonal antibody to insulin (1:100 dilution, H86; Santa Cruz Biotechnology) at 4°C overnight, followed by an Alexa Fluor 488 goat anti-rabbit IgG secondary antibody (1:100 dilution, ab150077; Abcam) and mounted with a mounting medium containing DAPI (VECTASHIELD; Vector Laboratories, Burlingame, CA). Fluorescent images were observed using an Eclipse 50i fluorescence microscope (Nikon, Melville, NY) and analyzed using SPOT 4.0 Advanced software (Diagnostic Instruments, Sterling Heights, MI).

Islet Tx Procedure and Post-Tx Treatment and Monitoring

For blood sampling, all animals had intravenous central lines placed 0–3 days before administration of STZ as previously reported (35). After the incubation with MN-siCas-3 or control probe, islets were transplanted into diabetic recipients. Treatment groups are presented in Table 1. The infusion procedure consisted of making an ~4-cm longitudinal incision in the abdomen ~3–4 inches lateral to midline. A short section of small bowel was then eviscerated, and a large mesenteric vein was identified. The vein was then cannulated with a 22-gauge angiocatheter, and the islets were then infused into the liver over the course of 5–10 min and the venotomy closed with one 7-0 Prolene suture. All recipients of allogeneic islets ($n = 6$) received a consistent number of islets (6,650–8,750 IEQ/kg), which is considered to be marginal (4). After the procedure, the animals were followed for 90 days as described below. Recipients in both groups were maintained on the identical immunosuppression protocol and displayed no statistical differences in the levels of tacrolimus ($P < 0.05$).

Immunosuppression

Induction therapy began on day −5 by injecting the recipients with a single dose of rituximab (10 mg/kg) (Rituxan; Genentech, South San Francisco, CA). On day −1, all recipient animals received a dose of rabbit antithymocyte globulin (10 mg/kg) (thymoglobulin; Sanofi Genzyme, Cambridge, MA) as well as continuous intravenous administration of tacrolimus (Astellas Pharma, Northbrook, IL) titrated to a therapeutic level of 10–15 ng/mL. On day 0, the animals were given daily 500 mg of mycophenolate mofetil (Genentech) per os and received a single intravenous dose of anti-CD40 monoclonal antibody (2C10R1, Recombinant; Nonhuman Primate Reagent Resource, Boston, MA) on postoperative days (PODs) 2, 5, and 11. Tacrolimus and mycophenolate mofetil were continued until the study end point (POD 90) (Fig. 1*B*).

Assessment of Clinical Parameters

To assess islet function, blood glucose was tested daily through tail stick using a glucometer. Liver function, serum creatinine, and complete blood count (CBC) tests were performed daily through venous draws off the central line. At POD 90, animals were sacrificed, and histological sections were obtained from the liver and pancreas and stained with hematoxylin-eosin and insulin.

Immunologic Assays

Antidonor responses were assessed by enzyme-linked immunospot assays (33) as well as by antidonor antibody flow cytometric analysis (FCM; BD Biosciences, San Jose, CA) before islet Tx as well as at 1 month and 2–3 months after islet Tx. Absolute T- and B-cell counts were assessed by FCM using anti-human CD3 (SP34-2; BD Biosciences), CD4 (SK3; BD Biosciences), CD8 (RPA-T8; BD Biosciences), and CD20 (LT20; Miltenyi Biotec, Bergisch Gladbach, Germany) monoclonal antibodies (33).

MRI

To confirm the presence of labeled islets in the baboon liver, we performed MRI on POD 2 as described previously (28). Before the procedure, the baboons were fasted for 8 h. The animals were then sedated with ketamine (10 mg/kg) and maintained on intravenous propofol sedation. The MRIs were acquired using a GoldSeal Signa HDxt 1.5T MRI scanner equipped with body matrix coil and spine array coil (GE Healthcare, Chicago, IL). Liver imaging sequences include T1-weighted image and T2* map. Imaging parameters were as follows (27): T1-weighted image (with respiratory gating), repetition time/echo time = 500/7.8 ms, slice thickness 3 mm, field-of-view (FOV) read = 180 mm, FOV phase = 100%, matrix size 192 × 192, flip angle = 50°, number of slices = 12, and number of averages = 4; T2* map (with respiratory gating), repetition time/echo time = 157/2.09–29.09 ms, slice thickness = 3 mm, FOV read = 200 mm, FOV phase = 100%, flip angle = 25°, number of slices = 10, and number of averages = 4. All images were processed using ImageJ software (1.48g; National Institutes of Health).

Statistical Analysis

Statistical analysis of the differences between the two groups was assessed by *t* test. Differences were considered statistically significant at $P < 0.05$. Sex was not considered a factor in the statistical analysis of the data because only one female animal was used (control animal 4515).

Data and Resource Availability

The data sets generated and/or analyzed during the current study are available from the corresponding author upon reasonable request. The theranostic probe MN-siCas-3 generated during the current study is available from the corresponding author upon reasonable request.

RESULTS

In Vitro Assessment of Islet Protection by MN-siCas-3

The islet purification procedure resulted in >80% viable, 90–95% high-purity islets. To test the protective effect of MN-siCas-3 probe on isolated islets, the islets were counted before and after being placed in culture with the

probes for 48 h. While in the control group we observed a 37.6 ± 15.0% reduction in islet yield after 48-h culture, in the experimental group, we observed a stark difference with only 12.0 ± 13.0% reduction ($P = 0.0172$).

We also directly assessed the in vitro antiapoptotic effects of the probes. After 48-h culture, we performed DNA isolation from cultured islets followed by apoptotic assay. Both the positive control lane and the control islets demonstrated smearing and laddering, indicative of DNA fragmentation as a result of apoptosis (Fig. 2*A*, lanes 1 and 2). However, the experimental islets demonstrated intact DNA, suggesting a direct protective effect of MN-siCas-3 (Fig. 2*A*, lane 3). Confirmation of MN-siCas-3 accumulation in baboon islets was further confirmed by fluorescence microscopy. Figure 2*B* shows excellent colocalization of the Cy5.5 signal with anti-insulin staining, thus providing direct evidence that the probe was taken up by islet cells (Fig. 2*B*).

Protective Effect of MN-siCas-3 on Transplanted Pancreatic Islets

The goal of this study was to demonstrate the protective effect of gene silencing on transplanted pancreatic islets. After labeling with either theranostic MN-siCas-3 or parental nanoparticles, islets were transplanted in the liver of diabetic baboons. MRI confirmed the presence of labeled islets after Tx (Fig. 3*A* and *B*, POD 2 is shown). In both cases, labeled islets appeared as dark voids of signal intensity on MRIs consistent with our previous findings (28). There was no difference in appearance of labeled islets on the images after labeling with either probe. However, there was a significant difference in the ability of differentially labeled islets to induce a protective effect. According to our experimental design (Fig. 1*B*), all animals received allogeneic islets in the marginal range of 6,650–8,750 IEQ/kg, and at the time of islet Tx, were requiring >10 units of insulin a day. Immediately after transplant, blood glucose levels in all baboons that received MN-siCas-3-labeled islets was reduced to the normal range and remained at 80–120 mg/dL most of the time (Fig. 4*A*–*D*). For the duration of the experiment, all animals in this experimental group had dramatically lower insulin requirements during transient blood glucose raise compared with pre-Tx. One animal (16P22) (Fig. 4*A*) remained completely insulin independent after Tx. The other three animals only required 0–1 or 1–2 units of insulin a day after Tx. In contrast, the control group demonstrated significant insulin requirements. Control animal 4515 had initial stable blood glucose levels but began to require exogeneous insulin on POD 10, ultimately needing a consistent 5–6 units a day until experimental end point (Fig. 5*A*). Blood glucose levels in another animal (16P46) (Fig. 5*B*) began to rise on POD 2, and as a result, this animal required consistent exogeneous insulin by POD 5. The animal's insulin requirement continued to rise, requiring 7–8 units/day by the experimental end point. Another confirmation that Tx is needed for restoration of normoglycemia was obtained with control animal 15P59, which did not receive islet infusion and developed respiratory complications secondary to diabetic ketoacidosis and insulin requirement of >16 units; this animal was euthanized 8 days after STZ bolus. Confirmation of STZ destruction of native pancreatic islets was obtained at necropsy, showing a small number of degenerated and scattered islets compared with healthy pancreatic tissue from a naive (unrelated) baboon (Supplementary Fig. 3). Analysis of C-peptide levels confirmed that STZ was successful in destroying the native islets (data not shown).

Histological Evaluation and Long-term Safety of MN-siCas-3 Probe

Upon completion of our experiments, we performed histology of the graft sections. First, we found that in all experimental animals on POD 90, there were larger and more frequent islet clusters in the portal veins compared with islets in control animals, which were small, dense, and scattered (Fig. 6*A* and *B*). Second, we observed that at the end point of the study, the livers of all the animals from

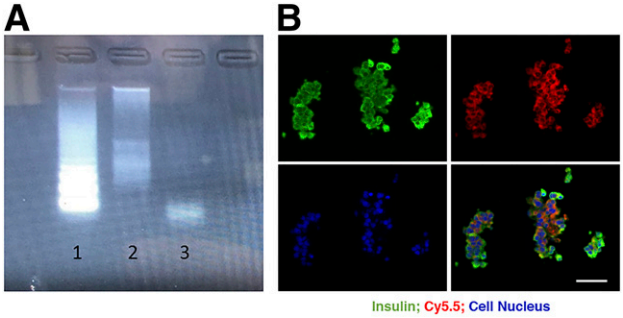

Figure 2—*A*: Apoptotic DNA Ladder Detection Assay demonstrated smearing and laddering in the positive control (lane 1) and the control (nonincubated) islets (lane 2), indicative of fragmentation of DNA caused by apoptosis. In contrast, islets incubated with MN-siCas-3 probe (lane 3) were devoid of these features, suggesting a protective effect of the probe. *B*: Fluorescence microscopy of baboon islets after incubation with MN-si-Cas-3 for 48 h (Cy5.5, insulin, DAPI cell nuclei). Colocalization of a Cy5.5 signal with anti-insulin staining provided direct evidence of the accumulation of nanoparticles in islet cells (magnification bar = 50 μm).

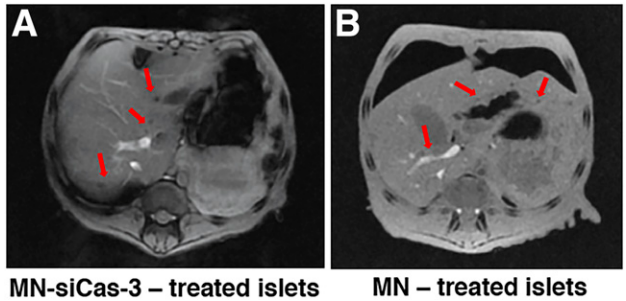

Figure 3—In vivo MRI of transplanted pancreatic islets labeled with MN-siCas-3 (*A*) or MN (*B*) probes. Islets appear as dark voids of signal intensity (arrows) on T2-weighted images.

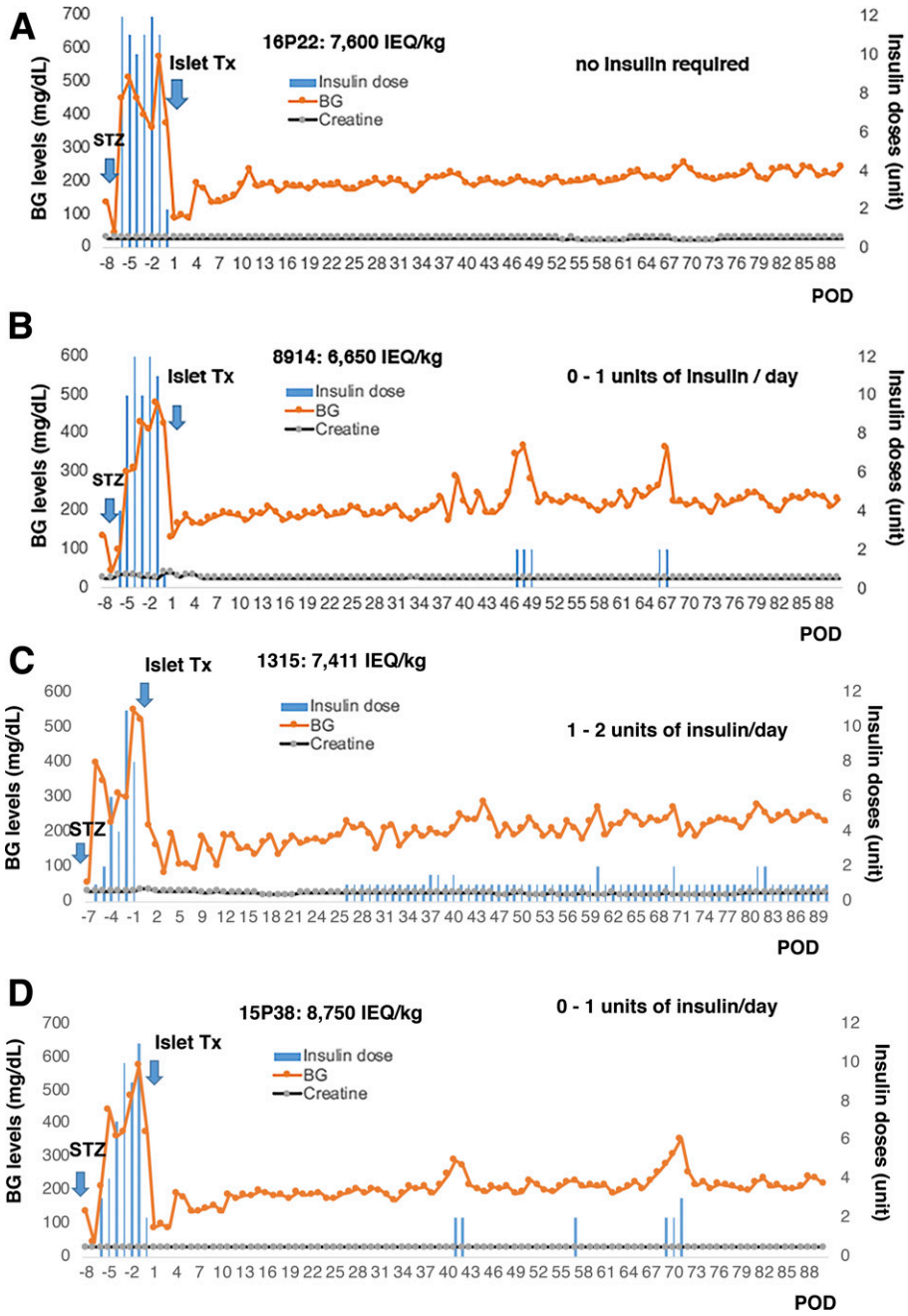

Figure 4—Daily blood glucose (BG) values and insulin units as a function of time for experimental animals show a significant decrease in insulin requirements. *A–D*: Data for individual animals are shown. Creatine levels are shown in Supplementary Fig. 5.

the experimental group had no remarkable morphological findings (Fig. 6*C*). In contrast, the livers of the control animals showed swelling and vacuolar degeneration of hepatic cells, which were evident in the pericentral zone of the hepatic lobes, similar to findings seen in the early phases of nonalcoholic steatohepatitis (Fig. 6*D*). This could be due to hepatic sinusoidal injury secondary to fatty infiltrate caused by the chronic hyperglycemia that these animals experienced. In addition, infusion of dying unprotected islets could cause local inflammation in the liver with the recruitment of inflammatory cells and cytokine production. Tests for liver function also showed elevated ALT values for at least one of the control animals (4515) at POD 50 (Supplementary Fig. 4*A*) that also had reduced hematocrit and platelet count (Supplementary Fig. 4*C*). Animals that received MN-siCas-3–labeled islets showed normal ALT levels except for one that had higher-than-normal values starting during the pre-Tx period (Supplementary Fig. 4*B*). CBC and creatinine levels were normal for both groups throughout the study (Supplementary Figs. 4*C* and *D* and 5, respectively).

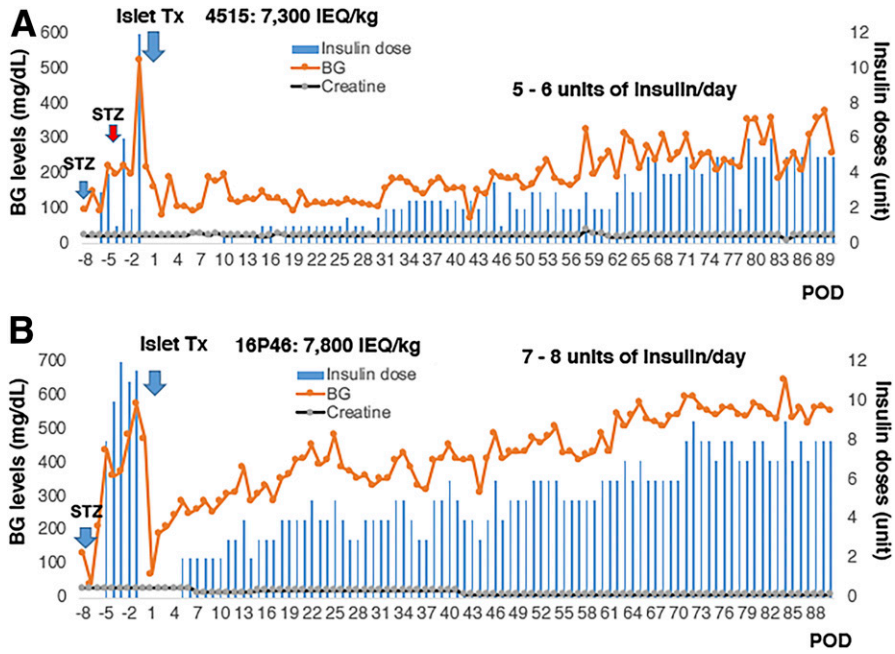

Figure 5—Daily blood glucose (BG) values and insulin units as a function of time for control animals show significantly higher insulin requirements compared with experimental animals. *A* and *B*: Data for individual animals are shown. Creatine levels are shown in Supplementary Fig. 5.

DISCUSSION

To date, whole-organ pancreas Tx remains the most durable long-term treatment modality for patients with diabetes (3,37); however, the procedure is associated with significant mortality and morbidity in the early Tx period (38,39). By its minimally invasive nature, islet Tx avoids the many surgical complications associated with whole-organ pancreas Tx (3). The major drawback, however, continues to be graft loss shortly after Tx, leading to recipients regaining their insulin dependence (2–4). Most importantly, multiple donors are needed for Tx in a single patient, resulting in a shortage of donor islets (40). To achieve the goal of islet Tx resulting in excellent glycemic control without severe hypoglycemia, significant efforts should be directed toward the reduction of islet damage during the immediate post-Tx period in conjunction with decreasing the number of islets required for a single recipient.

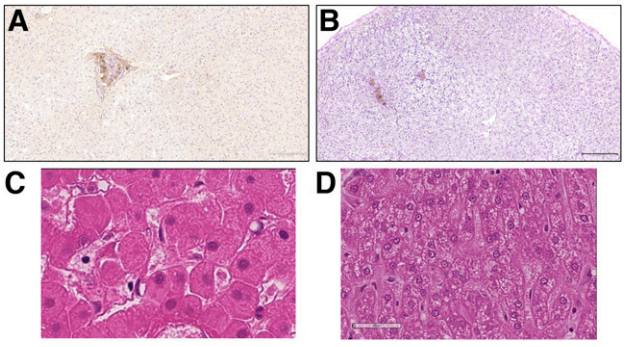

Figure 6—Histological evaluation. Insulin staining at necropsy showed significantly larger and more frequent islet clusters in the livers of experimental animals (*A*) compared with small, dense, and scattered islets found in control animals (*B*). Livers from the animals in the experimental group had no remarkable morphological findings (*C*), while livers from the control animals showed swelling and vacuolar degeneration of hepatic cells in the pericentral zone of the hepatic lobes (*D*). Scale bars = 200 μm (*A* and *B*) and 50 μm (*C* and *D*).

With these two goals in mind, we designed a set of experiments aimed at reducing post-Tx islet damage by utilizing RNA interference technology that would lead to islet protection from apoptosis as a result of various inflammatory events (41). In addition, we hypothesized that by protecting islets and supporting their viability, we could use a marginal number of islets required for each transplant. Our previous studies demonstrated successful application of this approach for reducing islet damage after Tx in small rodents (30,31). To improve the outcomes of clinical islet Tx and with the goal of clinical translation of our strategy, the next set of experiments was performed in a large animal (NHP) model.

We first performed in vitro studies on isolated baboon islets. Our results demonstrated that islet loss that normally already occurs during islet culture before Tx could be significantly reduced by incubating islets with the probe containing siRNA to caspase-3. This result was confirmed by two independent methods: counting viable islets before and after 48-h incubation and assessing DNA fragmentation using apoptotic assay. This difference in islet viability in vitro is compelling because it provides early evidence of

their durability after Tx in vivo. Moreover, it suggests the potential for other applications where there is a need to improve survival of living cells in the Tx setting.

For in vivo studies, we transplanted islets labeled with the theranostic MN-siCas-3 probe or parental nanoparticles in diabetic animals. Our results demonstrated a remarkable reduction in insulin requirements in all four animals in the experimental group compared with pre-Tx levels. One animal (16P22) achieved complete insulin independence for the duration of the experiment. Importantly, these animals received a marginal number of islets (6,650–8,750 IEQ/kg) that otherwise would not be sufficient to maintain normoglycemia. This was in stark contrast to the control group, where animals demonstrated significantly higher insulin requirements soon after receiving transplants. MRI of transplanted islets assisted in their visualization during the early post-Tx period and did not reveal any difference in their appearance.

Looking toward clinical translation of this procedure, we note that all animals tolerated their islet infusion well and exhibited a stable appetite and appropriate clinical behavior. Importantly, liver function, kidney tests, and CBCs were overall normal and similar between the two groups throughout the experiment. This suggests that the siRNA as part of the probe had no clinical impact on the animals' health after the infusion. Although there were no major laboratory abnormalities noted, there were gross changes in the livers of the control animals, including fatty infiltrates and vacuolar damage typically observed in patients with diabetes. These changes were absent in the experimental group.

Because donor shortage continues to hamper the outcome of islet Tx, researchers are searching for alternative sources of human islets as well as for alternative Tx sites that would increase islet survival. As such, some success has been achieved with porcine islets (42–44) and pluripotent stem cells (45–47). Similarly, alternative sites, such as bone marrow, omentum (48), muscle (49), or skin (50), have been tried with varying degrees of success. We believe that our approach in conjunction with in vivo imaging can protect and preserve precious islets from damage using an RNA interference mechanism that leads to stable control of blood glucose with a marginal number of islet cells and a drastic reduction in the amount of exogenous insulin. This also suggests the potential clinical usage of our technology toward living islet cell donors where reduction of the number of needed islets would reduce the amount of pancreas needed for donation, perhaps making living donation a clinical reality.

Funding. This work was supported in part by National Institutes of Health grants R01-DK-105503 and R01-DK-105468 to K.Y. and A.M.

Duality of Interest. No potential conflicts of interest relevant to this article were reported.

Author Contributions. T.P., P.W., K.T., K.M., Y.A., H.W., and A.S. researched the data and participated in the data analysis. T.P., P.W., K.Y., and A.M. participated in drafting the manuscript. X.C. performed islet isolation. N.R. synthesized and characterized the theranostic probe. K.Y. and A.M. designed the study, led the data analysis, and drafted the manuscript. A.M. conceived the idea. K.Y. and A.M. are the guarantors of this work and, as such, had full access to all the data in the study and take responsibility for the integrity of the data and the accuracy of the data analysis.

References

1. Shapiro AM. State of the art of clinical islet transplantation and novel protocols of immunosuppression. Curr Diab Rep 2011;11:345–354
2. Ryan EA, Paty BW, Senior PA, et al. Five-year follow-up after clinical islet transplantation. Diabetes 2005;54:2060–2069
3. Maffi P, Secchi A. Islet transplantation alone versus solitary pancreas transplantation: an outcome-driven choice? Curr Diab Rep 2019;19:26
4. Brennan DC, Kopetskie HA, Sayre PH, et al. Long-term follow-up of the Edmonton protocol of islet transplantation in the United States. Am J Transplant 2016;16:509–517
5. Barshes NR, Wyllie S, Goss JA. Inflammation-mediated dysfunction and apoptosis in pancreatic islet transplantation: implications for intrahepatic grafts. J Leukoc Biol 2005;77:587–597
6. Biarnés M, Montolio M, Nacher V, Raurell M, Soler J, Montanya E. Beta-cell death and mass in syngeneically transplanted islets exposed to short- and long-term hyperglycemia. Diabetes 2002;51:66–72
7. Bennet W, Groth CG, Larsson R, Nilsson B, Korsgren O. Isolated human islets trigger an instant blood mediated inflammatory reaction: implications for intraportal islet transplantation as a treatment for patients with type 1 diabetes. Ups J Med Sci 2000;105:125–133
8. Bottino R, Fernandez LA, Ricordi C, et al. Transplantation of allogeneic islets of Langerhans in the rat liver: effects of macrophage depletion on graft survival and microenvironment activation. Diabetes 1998;47:316–323
9. Davalli AM, Scaglia L, Zangen DH, Hollister J, Bonner-Weir S, Weir GC. Vulnerability of islets in the immediate posttransplantation period. Dynamic changes in structure and function. Diabetes 1996;45:1161–1167
10. Emamaullee JA, Stanton L, Schur C, Shapiro AM. Caspase inhibitor therapy enhances marginal mass islet graft survival and preserves long-term function in islet transplantation. Diabetes 2007;56:1289–1298
11. Huurman VA, van der Torren CR, Gillard P, et al. Immune responses against islet allografts during tapering of immunosuppression–a pilot study in 5 subjects. Clin Exp Immunol 2012;169:190–198
12. Moberg L, Johansson H, Lukinius A, et al. Production of tissue factor by pancreatic islet cells as a trigger of detrimental thrombotic reactions in clinical islet transplantation. Lancet 2002;360:2039–2045
13. Ricordi C, Strom TB. Clinical islet transplantation: advances and immunological challenges. Nat Rev Immunol 2004;4:259–268
14. Stadlbauer V, Schaffellner S, Iberer F, et al. Occurance of apoptosis during ischemia in porcine pancreas islet cells. Int J Artif Organs 2003;26:205–210
15. Niclauss N, Bosco D, Morel P, Giovannoni L, Berney T, Parnaud G. Rapamycin impairs proliferation of transplanted islet β cells. Transplantation 2011;91:714–722
16. Zahr E, Molano RD, Pileggi A, et al. Rapamycin impairs in vivo proliferation of islet beta-cells. Transplantation 2007;84:1576–1583
17. Monti P, Scirpoli M, Maffi P, et al. Islet transplantation in patients with autoimmune diabetes induces homeostatic cytokines that expand autoreactive memory T cells. J Clin Invest 2008;118:1806–1814
18. Gibly RF, Graham JG, Luo X, Lowe WL Jr., Hering BJ, Shea LD. Advancing islet transplantation: from engraftment to the immune response. Diabetologia 2011;54:2494–2505
19. Johnson JD, Ao Z, Ao P, et al. Different effects of FK506, rapamycin, and mycophenolate mofetil on glucose-stimulated insulin release and apoptosis in human islets. Cell Transplant 2009;18:833–845
20. Ricordi C, Zeng YJ, Alejandro R, et al. In vivo effect of FK506 on human pancreatic islets. Transplantation 1991;52:519–522

21. Zhang N, Su D, Qu S, et al. Sirolimus is associated with reduced islet engraftment and impaired beta-cell function. Diabetes 2006;55:2429–2436
22. Gala-Lopez BL, Neiman D, Kin T, et al. Beta cell death by cell-free DNA and outcome after clinical islet transplantation. Transplantation 2018;102:978–985
23. Emamaullee JA, Shapiro AM. Interventional strategies to prevent beta-cell apoptosis in islet transplantation. Diabetes 2006;55:1907–1914
24. Evgenov NV, Medarova Z, Dai G, Bonner-Weir S, Moore A. In vivo imaging of islet transplantation. Nat Med 2006;12:144–148
25. Evgenov NV, Medarova Z, Pratt J, et al. In vivo imaging of immune rejection in transplanted pancreatic islets. Diabetes 2006;55:2419–2428
26. Medarova Z, Evgenov NV, Dai G, Bonner-Weir S, Moore A. In vivo multimodal imaging of transplanted pancreatic islets. Nat Protoc 2006;1:429–435
27. Medarova Z, Vallabhajosyula P, Tena A, et al. In vivo imaging of autologous islet grafts in the liver and under the kidney capsule in non-human primates. Transplantation 2009;87:1659–1666
28. Wang P, Schuetz C, Vallabhajosyula P, et al. Monitoring of allogeneic islet grafts in nonhuman primates using MRI. Transplantation 2015;99:1574–1581
29. Medarova Z, Kumar M, Ng SW, et al. Multifunctional magnetic nanocarriers for image-tagged SiRNA delivery to intact pancreatic islets. Transplantation 2008; 86:1170–1177
30. Wang P, Yigit MV, Medarova Z, et al. Combined small interfering RNA therapy and in vivo magnetic resonance imaging in islet transplantation. Diabetes 2011;60: 565–571
31. Wang P, Yigit MV, Ran C, et al. A theranostic small interfering RNA nanoprobe protects pancreatic islet grafts from adoptively transferred immune rejection. Diabetes 2012;61:3247–3254
32. Moore A, Medarova Z. Imaging of siRNA delivery and silencing. Methods Mol Biol 2009;487:93–110
33. Tasaki M, Wamala I, Tena A, et al. High incidence of xenogenic bone marrow engraftment in pig-to-baboon intra-bone bone marrow transplantation. Am J Transplant 2015;15:974–983
34. Blanco CL, McGill-Vargas LL, McCurnin D, Quinn AR. Hyperglycemia increases the risk of death in extremely preterm baboons. Pediatr Res 2013;73:337–343
35. Yamada K, Hirakata A, Tchipashvili V, et al. Composite islet-kidneys from single baboon donors cure diabetes across fully allogenic barriers. Am J Transplant 2011;11:2603–2612
36. O'Neil JJ, Tchipashvili V, Parent RJ, et al. A simple and cost-effective method for the isolation of islets from nonhuman primates. Cell Transplant 2003;12:883–890
37. Dean PG, Kukla A, Stegall MD, Kudva YC. Pancreas transplantation. BMJ 2017;357:j1321
38. Kandaswamy R, Stock PG, Gustafson SK, et al. OPTN/SRTR 2017 Annual Data Report: pancreas. Am J Transplant 2019;19(Suppl. 2):124–183
39. Lombardo C, Baronti W, Amorese G, Vistoli F, Marchetti P, Boggi U. Transplantation of the pancreas. In *Endotext*. Feingold KR, Anawalt B, Boyce A, et al., Eds. South Dartmouth, MA, MDText.com, Inc., 2000
40. Anazawa T, Okajima H, Masui T, Uemoto S. Current state and future evolution of pancreatic islet transplantation. Ann Gastroenterol Surg 2018;3:34–42
41. Ramnath RD, Maillard E, Jones K, et al. In vitro assessment of human islet vulnerability to instant blood-mediated inflammatory reaction (IBMIR) and its use to demonstrate a beneficial effect of tissue culture. Cell Transplant 2015;24:2505–2512
42. Hering BJ, Wijkstrom M, Graham ML, et al. Prolonged diabetes reversal after intraportal xenotransplantation of wild-type porcine islets in immunosuppressed nonhuman primates. Nat Med 2006;12:301–303
43. Bottino R, Wijkstrom M, van der Windt DJ, et al. Pig-to-monkey islet xenotransplantation using multi-transgenic pigs. Am J Transplant 2014;14: 2275–2287
44. Shin JS, Kim JM, Kim JS, et al. Long-term control of diabetes in immunosuppressed nonhuman primates (NHP) by the transplantation of adult porcine islets. Am J Transplant 2015;15:2837–2850
45. Pagliuca FW, Millman JR, Gürtler M, et al. Generation of functional human pancreatic β cells in vitro. Cell 2014;159:428–439
46. Rezania A, Bruin JE, Arora P, et al. Reversal of diabetes with insulin-producing cells derived in vitro from human pluripotent stem cells. Nat Biotechnol 2014;32:1121–1133
47. Helman A, Melton DA. A stem cell approach to cure type 1 diabetes. Cold Spring Harb Perspect Biol. 2 March 2020 [Epub ahead of print]. DOI: 10.1101/cshperspect.a035741
48. Baidal DA, Ricordi C, Berman DM, et al. Bioengineering of an intraabdominal endocrine pancreas. N Engl J Med 2017;376:1887–1889
49. Rafael E, Tibell A, Rydén M, et al. Intramuscular autotransplantation of pancreatic islets in a 7-year-old child: a 2-year follow-up. Am J Transplant 2008;8:458–462
50. Pepper AR, Gala-Lopez B, Pawlick R, Merani S, Kin T, Shapiro AM. A prevascularized subcutaneous device-less site for islet and cellular transplantation. Nat Biotechnol 2015;33:518–523